Optical and Quantum Electronics (2005) 37:133–147
DOI 10.1007/s11082-005-1131-6

Analysis and design of efficient coupling in photonic crystal circuits

P. SANCHIS[1,*], J. MARTÍ[1], B. LUYSSAERT[2], P. DUMON[2], P. BIENSTMAN[2] AND R. BAETS[2]
[1]*Valencia Nanophotonics Technology Center, Universidad Politécnica de Valencia, Camino de Vera s/n, 46022 Valencia, Spain*
[2]*Department of Information Technology, Ghent University-IMEC, Sint-Pietersnieuwstraat 41, B-9000 Ghent, Belgium*
*(*author for correspondence: E-mail: pabsanki@ntc.upv.es)*

Abstract. A rigorous analysis and design of efficient coupling from photonic crystal (PhC) waveguides into conventional dielectric waveguides is reported. Closed-form expressions for the reflection and transmission matrices that completely characterize the scattering that occurs at the interface are derived based on an eigenmode expansion technique and a Bloch basis. Analytic expressions are used to analyze the reflection into PhC waveguides. We obtain that negligible reflection can be achieved by choosing a certain interface within a PhC unit cell. Furthermore, analytic expressions are used to design a novel and compact coupler structure in order to achieve high coupling efficiency when broad dielectric waveguides are considered. Thereby, transmission efficiencies near 100% from the fundamental guided Bloch mode into the fundamental waveguide mode are achieved.

Key words: eigenmode expansion, electromagnetic scattering by periodic structures, mode-matching, photonic crystals

1. Introduction

Photonic crystals (PhC) have been the subject of an increasing research effort in order to develop micro-scale photonic integrated circuits (Joannopoulos *et al.* 1995). However, efficient coupling into and out of PhC circuits is one of the main challenges to achieve reliable micro-scale photonic integrated circuits based on the PhC technology. Coupling losses between conventional dielectric waveguides and PhC waveguides originate from the mode mismatch between both types of waveguides. Waveguides in PhC circuits are usually formed by inserting line defects into the otherwise periodic structure. The creation of a line defect results in guided modes within the photonic band gap (PBG), whose propagation is determined by the Bloch theorem (Bloch 1928). On the other hand, propagation in conventional dielectric waveguides relies on index-contrast guiding. At the moment, coupling losses in PhC circuits have mainly been studied by means of simulations, while theoretical work remains very scarce, (Palamaru and Lalanne 2001; Botten *et al.* 2003; Ushida *et al.* 2003; Biswas *et al.* 2004; Sanchis *et al.* 2004). However, the knowledge of analytic expressions for the transmission and

reflection at an interface between an external medium and a PhC circuit can be very useful when testing novel designs and studying the influence of different parameters on the coupling efficiency. Analytic expressions can dramatically reduce the computing time, by avoiding complex numerical simulations, which usually require huge computational resources. Recently, closed-form expressions based on an eigenmode expansion technique were derived for an interface between a dielectric waveguide and a semi-infinite PhC waveguide (Sanchis *et al.* 2004).

In this paper, transmission and reflection matrices are obtained for the (reverse) interface between a semi-infinite PhC waveguide and a dielectric waveguide as shown in Fig. 1(a). Contrasting with the previous work, in this case both forward and backward propagating Bloch modes inside the PhC waveguide need to be considered. Once analytic expressions are derived, they are first used to analyze the reflection into the PhC waveguide considering different interfaces between the dielectric and PhC waveguide, which are obtained by different cut positions that can be chosen within the basic period of the PhC. We found that the cut position that provides maximum transmission efficiency is not necessarily the same that provides minimum reflection into the PhC waveguide. Furthermore, negligible reflection is obtained at a certain cut position for a particular PhC structure which can be useful to avoid Fabry-Perot resonances in the transmission spectrum of PhC structures of finite length. Analytic expressions are also used to analyze the transmission efficiency for different dielectric waveguide widths. We obtain that the transmission efficiency is rather low, even choosing the optimum cut position, when broad dielectric waveguides are considered. However, a novel and compact coupler is proposed in order to improve the transmission efficiency up to nearly 100%. Basically, the coupler structure converts a multimode excitation with a high efficiency into a single-mode excitation of the dielectric waveguide. The limitations of the proposed coupler structure are also discussed.

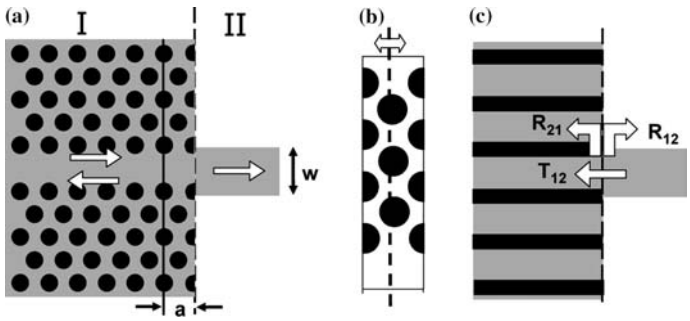

Fig. 1. (a) Analyzed structure where w is the width of the dielectric waveguide and a is the lattice constant, (b) supercell used to calculate the Bloch modes and (c) definition of R_{12}, R_{21} and T_{12}.

2. Interface between photonic crystal and dielectric waveguides

Figure 1(a) shows the analyzed interface formed by a line defect PhC waveguide butt-coupled to a dielectric waveguide. The transmission and reflection matrices are calculated by using the well known mode matching technique (Zaki *et al.* 1988). Therefore, we consider that an interface is placed at $z = 0$ and a single Bloch mode with index p is incident from medium I. This incident mode will give rise to a reflected field in medium I and a transmitted field in medium II. We expand the fields in terms of the Bloch modes in medium I and in terms of the eigenmodes in medium II. Imposing the continuity of the tangential components of the total field at the interface yields

$$E_p^{\mathrm{I}+} + \sum_j R_{j,p} E_j^{\mathrm{I}-} = \sum_j T_{j,p} E_j^{\mathrm{II}}, \tag{1}$$

$$H_p^{\mathrm{I}+} + \sum_j R_{j,p} E_j^{\mathrm{I}-} = \sum_j T_{j,p} H_j^{\mathrm{II}}, \tag{2}$$

where $E^{\mathrm{I}+}$, $H^{\mathrm{I}+}$, $E^{\mathrm{I}-}$, $H^{\mathrm{I}-}$ are the tangential electric and magnetic fields of the forward and backward propagating Bloch modes, respectively, and T and R are the transmission and reflection coefficients. In order to distinguish the forward propagating Bloch modes from the backward propagating Bloch modes we look at the power flux for the guided mode and at the imaginary part of the wave vector for the evanescent modes (Botten *et al.* 2001).

The unknown transmission and reflection coefficients are calculated by taking the right-cross product of (1) with H_i^{II} and the left-cross product of (2) with E_i^{II}, which are the expansion fields of medium II. Here, i is an arbitrary index. After integrating over the cross-section and by invoking the orthogonality relation in medium II, we get

$$\left\langle E_p^{\mathrm{I}+}, H_i^{\mathrm{II}} \right\rangle + \sum_j R_{j,p} \left\langle E_j^{\mathrm{I}-}, H_i^{\mathrm{II}} \right\rangle = T_{i,p} \langle E_i^{\mathrm{II}}, H_i^{\mathrm{II}} \rangle, \tag{3}$$

$$\left\langle E_i^{\mathrm{II}}, H_p^{\mathrm{I}+} \right\rangle + \sum_j R_{j,p} \left\langle E_i^{\mathrm{II}}, H_j^{\mathrm{I}-} \right\rangle = T_{i,p} \langle E_i^{\mathrm{II}}, H_i^{\mathrm{II}} \rangle, \tag{4}$$

where the scalar product is defined as the following overlap integral

$$\langle E_n, H_m \rangle = \int\!\!\int_S (E_n \times H_m) \mathrm{u}_z \, \mathrm{d}s.$$

The reflection can be easily obtained by subtracting (3) and (4) yielding

$$\left\langle E_p^{\mathrm{I}+}, H_i^{\mathrm{II}} \right\rangle - \left\langle E_i^{\mathrm{II}}, H_p^{\mathrm{I}+} \right\rangle = \sum_j R_{j,p} \left(\left\langle E_j^{\mathrm{I}-}, H_i^{\mathrm{II}} \right\rangle - \left\langle E_i^{\mathrm{II}}, H_j^{\mathrm{I}-} \right\rangle \right). \tag{5}$$

This equation can be simplified by decomposing the Bloch modes in terms of their forward, F_{k}, and backward, B_{k}, components. It should be noticed that the forward and backward components are different for the forward and backward propagating Bloch modes. Furthermore, the forward and backward components depend on the chosen cut position within the basic period of the PhC waveguide, as shown in Fig. 1(b). The chosen cut position will determine the index profile of the interface layer in medium I, shown at the left side in Fig. 1(c). Therefore, we get

$$\begin{aligned} \left\langle E_j^{\mathrm{I}+}, H_i^{\mathrm{II}} \right\rangle - \left\langle E_i^{\mathrm{II}}, H_j^{\mathrm{I}+} \right\rangle = & \sum_k F_k^{j+} \cdot \left(\left\langle \tilde{E}_{\mathrm{k}}, H_i^{\mathrm{II}} \right\rangle - \left\langle E_i^{\mathrm{II}}, \tilde{H}_{\mathrm{k}} \right\rangle \right) \\ & + \sum_k B_k^{j+} \cdot \left(\left\langle \tilde{E}_{\mathrm{k}}, H_i^{\mathrm{II}} \right\rangle + \left\langle E_i^{\mathrm{II}}, \tilde{H}_{\mathrm{k}} \right\rangle \right), \end{aligned} \tag{6}$$

where $\tilde{E}_k$ and $\tilde{H}_k$ are the electric and magnetic field of the interface layer. Equation (6) can be expressed with the following matrix equation

$$\left\langle E_j^{\mathrm{I}+}, H_i^{\mathrm{II}} \right\rangle - \left\langle E_i^{\mathrm{II}}, H_j^{\mathrm{I}+} \right\rangle \equiv 2(R_{12} T_{12}^{-1} F_+ + T_{12}^{-1} B_+), \tag{7}$$

where T_{12} and R_{12} are defined as shown in Fig. 1(c). It should be noticed that these terms are the same as those used in (Sanchis *et al*. 2004). A similar expression can be obtained for the right-hand side of (5) so that we obtain

$$-2(R_{12} T_{12}^{-1} F_+ + T_{12}^{-1} B_+) = 2(R_{12} T_{12}^{-1} F_- + T_{12}^{-1} B_-) R \tag{8}$$

that results in the reflection matrix

$$R = -(B_- - R_{21} F_-)^{-1} (B_+ - R_{21} F_+). \tag{9}$$

The transmission matrix is obtained by summing (3) and (4) and following a similar procedure as the one used above

$$T = T_{12}^{-1} (F_+ - R_{21} B_+) + T_{12}^{-1} (F_- - R_{21} B_-) R. \tag{10}$$

Thereby, the transmission and reflection matrices calculated with (10) and (9) completely characterize the scattering that occurs at the interface between a PhC waveguide and a dielectric waveguide. These matrices involve the

scattering properties of guided, radiation and evanescent modes. Thus, the transmitted and reflected power of the fundamental guided propagating Bloch mode into the i-mode of the dielectric waveguide is given by

$$\eta_T = |T_{i,0}|^2, \tag{11}$$

$$\eta_R = |R_{i,0}|^2, \tag{12}$$

where $T_{i,0}$ and $R_{i,0}$ are the i-row and first column of (10) and (9), respectively, and it is assumed that the modes are normalized.

3. Low reflection into photonic crystal waveguides

Based on reciprocity theorem, the transmission matrix that characterizes the transmission from the dielectric waveguide into the PhC waveguide is equal to the transposed of the transmission matrix that characterizes the transmission from the PhC waveguide into the dielectric waveguide. However, the reflection is usually different in both cases. Therefore, the transmission efficiency from the fundamental mode of the dielectric waveguide into the fundamental guided Bloch mode and vice versa will be the same while the reflection will be different. In this section, both types of reflection are analyzed.

The analytic results were obtained with a frequency-domain model based on a vectorial eigenmode expansion technique and a staircase approximation of the index profile (Bienstman 2001). This modeling tool CAMFR is freely available from the Internet (http://camfr.sourceforge.net). For the PhC waveguide, the Bloch modes were calculated from the eigenstates of the scattering matrix associated with the basic period. Afterwards, the field profiles and the forward and backward components of the Bloch modes were obtained at the chosen cut position within the basic period (Casey *et al.* 2004). The PhC structure considered is a two-dimensional triangular lattice of dielectric rods of Silicon ($n_{\mathrm{Si}} = 3.4$) surrounded by a homogeneous dielectric medium of silica ($n_{\mathrm{SiO_2}} = 1.45$). The radius of the rods is $0.2a$ where a is the lattice constant. The dielectric waveguide has a thickness of 0.5 μm and a core of Silica surrounded by a cladding of air. The PhC waveguide is formed by removing a line of rods and the frequency of operation is $0.3(a/\lambda)$ for TM polarized waves.

Figure 2(a) shows the transmission efficiency as a function of the chosen cut position within the basic period calculated with (11). The transmission efficiency varies along the different cut positions due to the variation of the modal properties of the Bloch modes. It can be seen that the result shown in Fig. 2(a) is in agreement with that reported in Sanchis *et al.* (2004) as

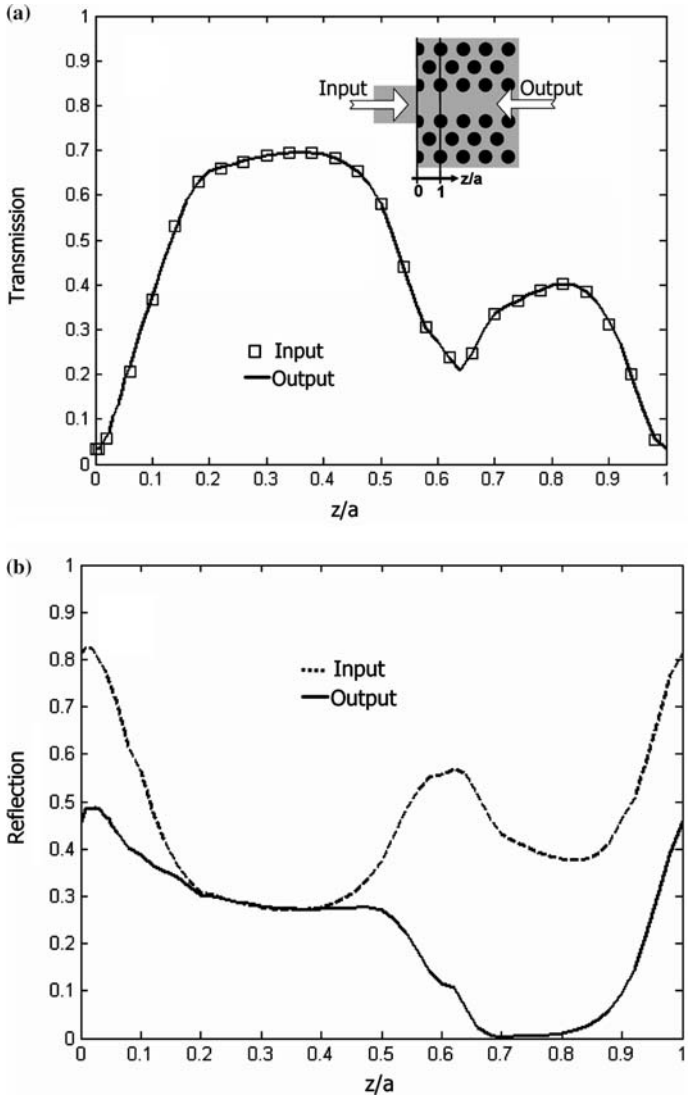

Fig. 2. (a) Transmission and (b) reflection as a function of the chosen cut position normalized by the lattice constant. The reflection is different depending on if the light is introduced or extracted from the photonic crystal.

expected from the reciprocity theorem. However, Fig. 2(b) shows the reflection as a function of the chosen cut position for two different cases: (i) input coupling where the light is propagated from the dielectric waveguide into the PhC waveguide and (ii) output coupling where the light is propagated from the PhC waveguide into the dielectric waveguide. In the former the reflection is calculated with the analytic expression derived in Sanchis *et al.* (2004) while in the latter it is calculated with (12). It is

important to notice that the reflection for the input coupling case is into the dielectric waveguide while the reflection for the output coupling case is into the PhC waveguide. From the results shown in Fig. 2(b), it can be seen that the reflection is different for both cases except for the range of z/a between 0.2 and 0.4 which corresponds with the range where the transmitted power is maximum (see Fig. 2(a)). However, the minimum reflection for the output coupling case is not achieved for the maximum transmission. The former is obtained at $z/a = 0.7$ while the latter is obtained at $z/a = 0.3$.

Figure 3 shows the reflection spectra for the input and output coupling cases at the cut positions which give the minimum reflection into the PhC waveguide ($z/a = 0.7$) and the maximum transmission efficiency ($z/a = 0.3$). The transmission efficiency at $z/a = 0.3$ is around 70% while the reflection into the dielectric waveguide (input coupling) is around 30%. Therefore, coupling losses are mainly due to reflection, while scattering losses are negligible. Scattering losses are due to the coupling to radiation modes which can only be excited in the dielectric waveguide. Therefore, it can be expected that radiation modes will also not be excited at the output coupling which could explain the similarity of the reflection spectra between both input and output coupling. However, a higher mode mismatch occurs at $z/a = 0.7$ which significantly increases the coupling to radiation modes, i.e. scattering losses. In this case, the transmission is around 30% while the reflection into the dielectric waveguide is around 40% so that scattering losses will be around 30%. Therefore, a high coupling to radiation modes can be expected for the output coupling, which could explain the very low reflection achieved into the PhC waveguide.

The minimization of the reflection that occurs when the light is extracted from the PhC waveguide can be useful to avoid Fabry-Perot resonances in the transmission spectrum of PhC structures of finite length. However, the transmission efficiency is reduced so a trade-off between maximum transmission and low reflection will exist. Figure 4 shows the transmission efficiency as a function of the normalized frequency for $z/a = 0.3$ and $z/a = 0.7$ and considering a semi-infinite PhC waveguide. Figure 5(a) shows the examined PhC structure of finite length where the optimum cut positions must be designed in both input and output interfaces. The transmission efficiency as a function of the normalized frequency for this PhC structure is shown in Fig. 5(b) for different cut positions at both input and output interfaces. The transmission spectra were calculated by means of FDTD simulations (Taflove 1995). An incident pulsed field was launched at an input dielectric waveguide so that the transmission spectrum was calculated with the overlap integral between the launched and measured field at the input and output dielectric waveguides, respectively.

When the input and output interfaces are chosen to achieve the maximum transmission efficiency ($z/a_{\text{in}} = z/a_{\text{out}} = 0.3$), notable Fabry-Perot resonances appear in the transmission spectrum as the reflection into the PhC waveguide

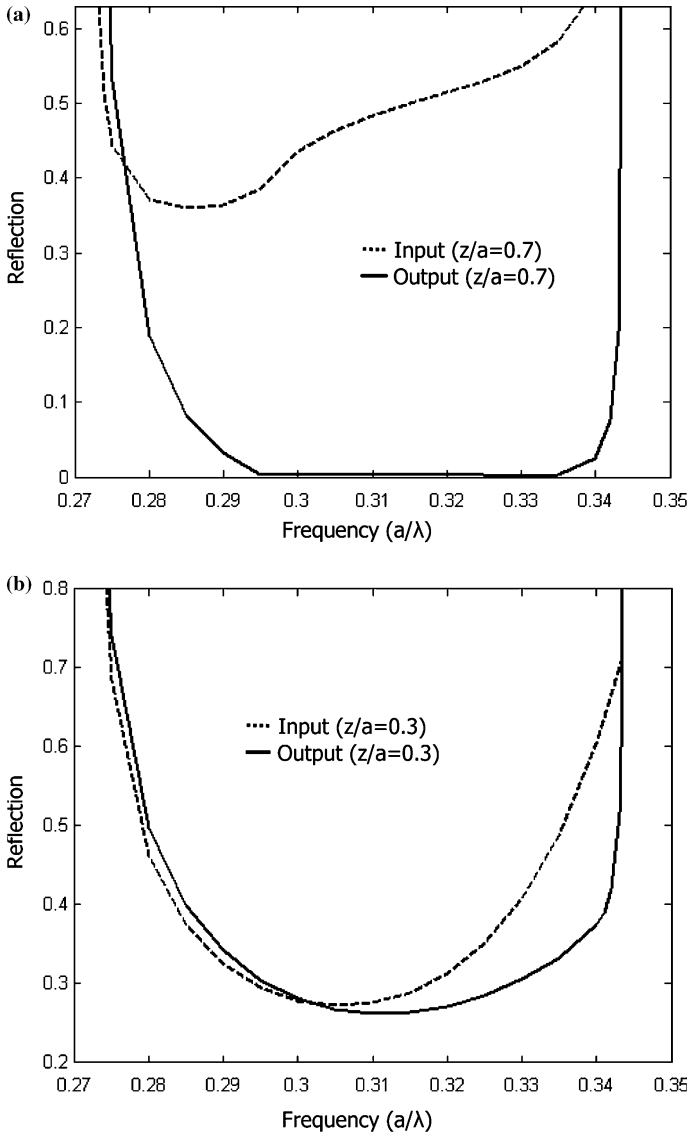

Fig. 3. Reflection as a function of the normalized frequency for the input and output coupling at (a)$z/a = 0.7$ and (b) $z/a = 0.3$.

is significant. It can be seen that the transmission at the resonance peaks is near unity at the frequencies where scattering is negligible. In the second case, the input and output interfaces are chosen to minimize the reflection into the PhC waveguide ($z/a_{\text{in}} = z/a_{\text{out}} = 0.7$). In this case, it can be seen that the Fabry-Perot resonances are eliminated but the overall transmission efficiency is very low. One possible approach to improve the transmission efficiency

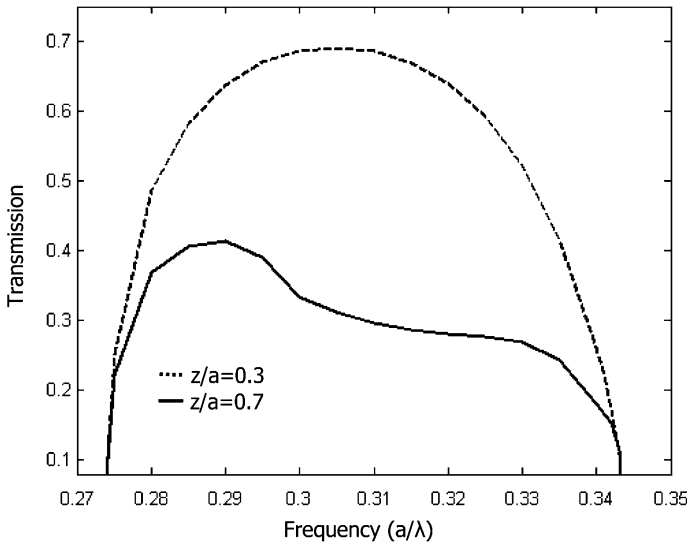

Fig. 4. Transmission efficiency as a function of the normalized frequency for different cut positions.

without increasing Fabry-Perot resonances is to use at the output interface the cut position which gives minimum reflection into the PhC waveguide ($z/a_{\text{out}} = 0.7$) and use at the input interface the cut position which gives maximum transmission ($z/a_{\text{in}} = 0.3$). Thus, the transmission efficiency is improved without increasing the Fabry-Perot peaks as the reflection at the output interface is still negligible. However, it can be seen that some resonances appear at the frequency range between $0.275(a/\lambda)$ and $0.3(a/\lambda)$ which is in agreement with the increase in reflection that can be seen in Fig. 3(a). Finally, we want to remark that the agreement between FDTD results and the analytic results for the corresponding semi-infinite PhC structure demonstrate the validity of the analytic expressions derived in the previous section.

4. High transmission efficiency into broad dielectric waveguides

The transmission efficiency decreases as broader dielectric waveguides are used due to the higher mode mismatch which mainly stems from the mode profile mismatch. Figure 6(a) shows the transmission into the fundamental mode of the dielectric waveguide as a function of the chosen cut position for three different dielectric waveguide widths: 0.5, 1.5 and 2 μm. In this case, a PhC structure formed by air holes in a dielectric medium of Silicon has been considered. The dielectric waveguide also has a core of Silicon surrounding by an air cladding. We use the effective index approximation ($n_{\text{eff}} = 2.7$) and a hole radius of $0.3a$. The PhC waveguide is formed by removing a line of holes and the frequency of operation is 0.3 (a/λ) for TE polarized waves.

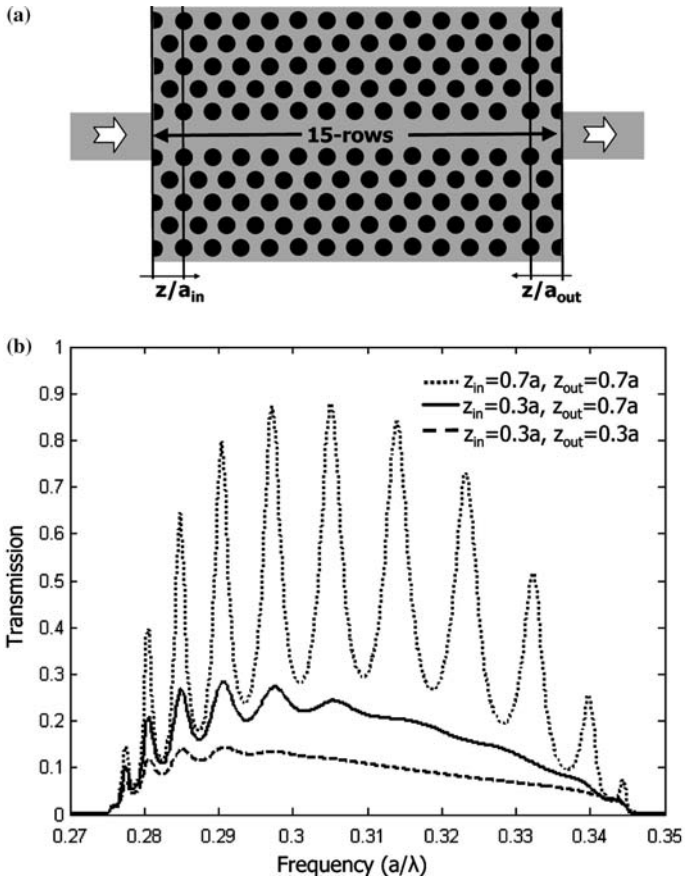

Fig. 5. (a) PhC structure of finite length considered and (b) corresponding transmission efficiency as a function of the normalized frequency calculated by means of FDTD simulations.

In Fig. 6(a), it can be seen that although high transmission can be achieved with this kind of PhC structure when narrow dielectric waveguides are used, the transmission significantly decreases when broader dielectric waveguides are considered even by choosing the optimum cut position. For a width of 2 μm, the maximum transmission efficiency is only of 67% for the optimal cut position ($z/a = 0.3$). However, the reflection into the PhC waveguide, shown in Fig. 6(b), is maintained below 1% even when broad dielectric waveguides are considered. This means that almost all the power is transmitted out of the PhC waveguide. However, the low transmission into the fundamental mode of the dielectric waveguide indicates that higher transmission occurs to the higher order guided modes as well as to radiation modes which can both be excited in the dielectric waveguide. It is important to notice that the number of guided modes that the dielectric waveguide supports increases as the waveguide width increases. For the waveguide

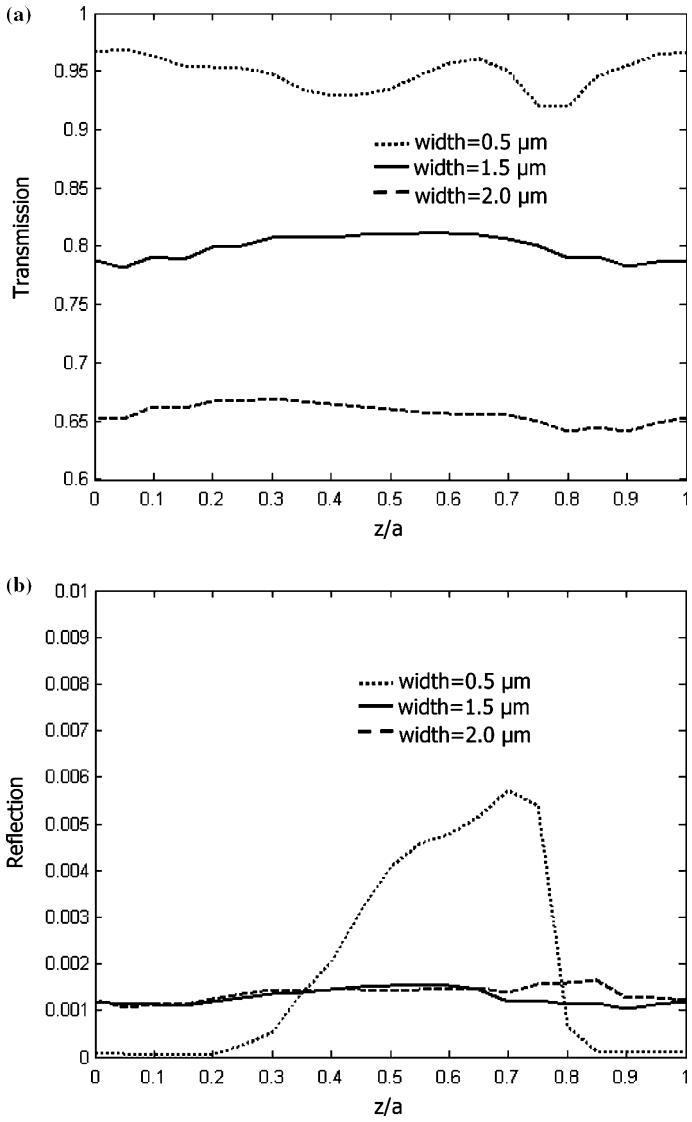

Fig. 6. (a) Transmission and (b) reflection into the PhC waveguide as a function of the chosen cut position and for different dielectric waveguide widths. The PhC structure in this case is formed by air holes in a dielectric background.

widths shown in Fig. 6, only the narrower waveguide with a width of 0.5 μm has one even guided mode. However, three and four even guided modes can be excited in the 1.5 and 2 μm-wide waveguides, respectively.

There are several approaches to increase the transmitted power into and out of PhC waveguides using broad dielectric waveguides. However, they can be roughly separated in two groups which differ on if the PhC structure is

altered at the interface, for instance using PhC tapers (see e.g. Sanchis *et al.* 2002) or if the dielectric waveguide structure is altered at the interface. In the latter, the simpler approach is to use the widely studied dielectric tapers (see e.g. Murphy 1988) in which the width of a broader waveguide is adiabatically varied up to a narrower width. In this case, the narrower width will be chosen in order to achieve the maximum coupling efficiency into the PhC structure. However, this approach requires long structures to obtain high transmission. For the PhC structure considered, a 5 μm-long linear taper was firstly used to couple a 2 μm-wide waveguide with the PhC waveguide. The linear taper reduces the waveguide width from 2 to 0.5 μm. Furthermore, the optimum cut position which gives maximum transmission, $z/a = 0.95$, has been chosen to couple the 0.5 μm-wide dielectric waveguide with the PhC waveguide. Figure 7 shows the magnetic field diagram for the long taper used for coupling into and out a PhC waveguide of finite length. In this case, a transmission of 95% for the fundamental mode is achieved from the input to the ouput dielectric waveguide. However the transmission is drastically reduced to 57% when a 1.4 μm-long linear taper is used. Figure 8 shows the magnetic field diagram when the short taper is used.

A novel and compact coupler is proposed to improve the coupling. Figure 9 shows the magnetic field diagram for the designed coupler structure used to couple light into and out the same PhC waveguide of finite length. The coupler length is 1.4 μm. The procedure to design the coupler was the following. Firstly, the amplitude and phase of the transmission coefficients corresponding to the guided modes of the dielectric waveguide were calculated with (10) at the optimum cut position ($z/a = 0.3$). Then, the coupler structure was designed, regardless of the PhC structure, by means of a genetic algorithm (Michalewicz and Fosel 1998) in order to convert the multimode excitation into a single-mode excitation. The coupler consists of 14 sections with a length of 0.1 μm. The widths of these sections form the input of the optimization algorithm. A transmission efficiency of 98% for the fundamental mode is achieved from the input to the output dielectric waveguide. The obtained coupler structure shows very small wing-like features, in which

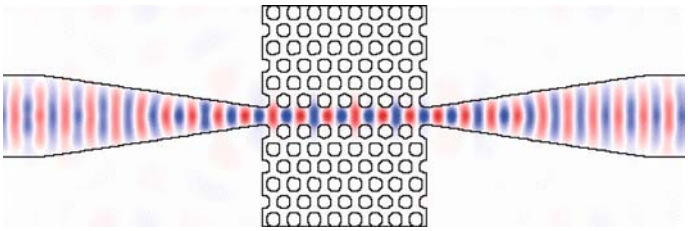

Fig. 7. Magnetic field diagram for the 5 μm-long linear used for coupling into and out a PhC waveguide of finite length using a 2 μm-wide dielectric waveguide.

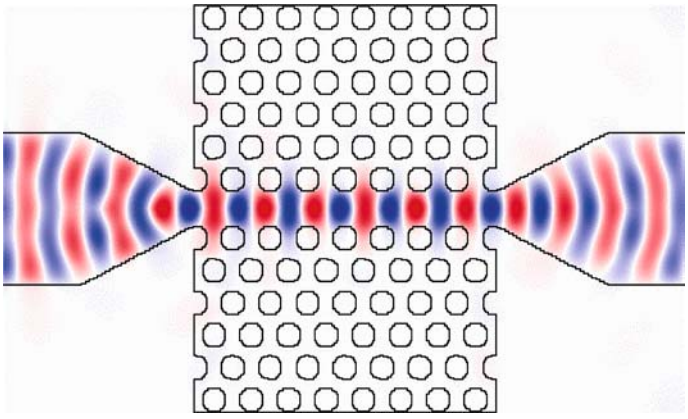

Fig. 8. Magnetic field diagram for the 1.4 μm-long linear used for coupling into and out a PhC waveguide of finite length using 2 μm-wide dielectric waveguide.

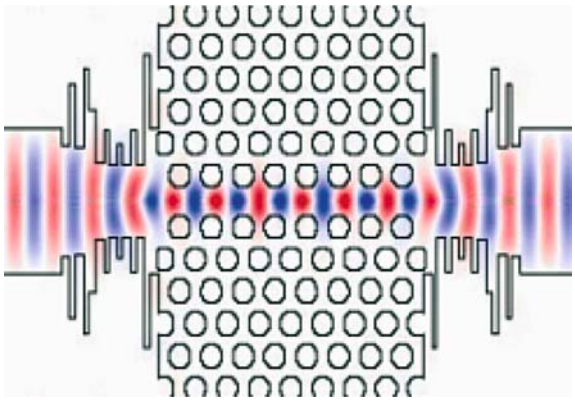

Fig. 9. Magnetic field diagram for the 1.4 μm-long compact coupler used for coupling into and out a PhC waveguide of finite length using a 2 μm-wide dielectric waveguide.

the magnetic field has a small value. Although their exact role has not yet been determined, they are necessary for the structure to function well. When the three middle wing-like waveguide sections are replaced by sections with a width that is the average width of the two neighbouring sections, the overall transmission efficiency of the structure drops below 80%. Figure 10 shows the butt coupling case in which a transmission efficiency of only 41% is achieved, even using the optimum cut position. Furthermore, it can be seen that the magnetic field has a complex pattern due to the high reflection and interaction between the multiple guided modes.

We also tried to repeat a similar design for coupling to the rod PhC structure considered in Section 3 using a broader dielectric waveguide. The problem was that in this case most of the power was scattered into radiation

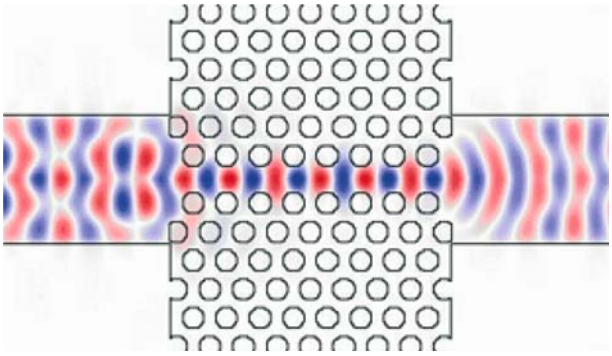

Fig. 10. Magnetic field diagram for the butt-coupling between a 2 μm-wide dielectric waveguide and the PhC waveguide of finite length.

modes mainly due to the low index contrast of the dielectric waveguide. Therefore, the transmitted power was not significantly improved regarding the butt-coupling structure. In conclusion, high transmission efficiency is achieved with the proposed coupler structure when almost all the power is scattered into the guided modes of the dielectric waveguide that means that the reflection into the PhC waveguide has to be very low as well as the coupling to the radiation modes which can be excited in the dielectric waveguide. In this context, the obtained analytic expressions are a useful instrument for efficiently testing different dielectric and PhC structures avoiding complex and huge time consuming simulations.

5. Conclusions

Closed-form expressions for the reflection and transmission matrices at the interface between a PhC structure and an external medium have been derived. The obtained formulas in addition to those obtained in Sanchis *et al.* (2004) can be very useful for completely analyzing the influence of different parameters on the coupling efficiency as well as for efficiently helping in the design of novel structures.

We have also shown that the reflection into a PhC waveguide can be minimized by using the appropriate cut position chosen within the basic period of the PhC. Furthermore, a compact coupler structure has been proposed in order to improve the coupling efficiency when broad dielectric waveguides are used. The proposed coupler structure converts a multi-mode excitation into a single-mode excitation. Therefore, transmission efficiencies near 100% from the fundamental guided Bloch mode into the fundamental mode of the dielectric waveguide can be achieved.

Finally, we want to point out that only two-dimensional problems have been considered here. However, analytic expressions can also be used for three-dimensional (3D) problems in which the advantages when comparing with conventional numerical simulations, such as FDTD, will be much more noteworthy. In this case, only the 3D calculation of the Bloch modes of the corresponding PhC waveguide as well as the 3D calculation of the dielectric waveguide modes is required in order to use analytic expressions.

Acknowledgements

This work has been partially funded by the Spanish Ministry of Science and Technology under grant TIC2002-01553. Parts of this work were also performed in the context of the Belgian DWTC project IAP-Photon. P. Sanchis acknowledges the Spanish Ministry of Education, Culture and Sport for funding his grant. P. Bienstman acknowledges the Flemish Fund for Scientific Research (FWO-Vlaanderen) for a postdoctoral fellowship. B. Luyssaert and P. Dumon acknowledge the Flemish Institute for the Industrial Advancement of Scientific and Technological Research (IWT) for a specialization grant.

References

Bloch, F. *Z. Physik*. **52** 555, 1928.
Bienstman, P. *Ph.D. dissertation*, Ghent University, Belgium, 2001.
Biswas, R., Z.Y. Li and K.M. Ho. *Appl. Phys. Lett*. **84**(8) 1254, 2004.
Botten, L.C., N.A. Nicorovici, R.C. McPhedran, C. Martijn de Sterke and A.A. Asatryan. *Phys. Rev. E* **64** 046603, 2001.
Botten, L.C., A.A. Asatryan, T.N. Langtry, T.P. White, C. Martijn de Sterke and R.C. McPhedran. *Opt. Lett*. **28**(10) 854, 2003.
Casey, K.H., E. Lidorikis, X. Jiang, J.D. Joannopoulus, K.A. Nelson, P. Bienstman and S. Fan. *Phys. Rev. B* **69** 195111, 2004.
Joannopoulos, J.D., R.D. Meade and J.N. Winn. *Photonic Crystals*. Princeton University Press, Princeton, NJ, 1995.
Michalewicz, Z. and D.B. Fogel. *How to solve it: Modern Heuristics*, Springer, Berlin, 1998.
Murphy, E.J. *IEEE J. Light. Tech*. **6** 862, 1998.
Palamaru, M. and P. Lalanne, *Appl. Phys. Lett*. **78** 1466, 2001.
Sanchis, P., J. Martí, J. Blasco, A. Martínez, and A. García. *Opt. Express* **10** 1391, 2002.
Sanchis, P., P. Bienstman, B. Luyssaert, R. Baets and J. Marti. *IEEE J. of Quantum Electro*. **40**(5) 541, 2004.
Taflove, A. *Computational Electrodynamics*, Norwood, MA, Artech, 1995.
Ushida, J., M. Tokushima, M. Shirane, A. Gomyo and H. Yamada. *Phys. Rev. B* **68** 155115, 2003.
Zaki, K.A., S. Chen, and C. Chen. *IEEE Trans. Microwave Theor. Tech*. **36** 1804, 1988.